

Supplementary Information

Dynamic Polyimine Networks with Good Malleability and Closed-Loop Recyclability from Upcycled Poly(ethylene terephthalate) Waste

Mengzhe Han,^a Ying Zheng,^{*,a,b} Maolin Li,^a Xing Zhang,^a, Jing Li,^a Chengtao Yu,^{a,b}
Junfeng Liu,^{a,b} Guorong Shan^{a,b}, Yongzhong Bao^{a,b}, and Pengju Pan^{*,a,b}

^a *State Key Laboratory of Chemical Engineering and Low-Carbon Technology, Key Laboratory of Biomass Chemical Engineering of Ministry of Education, College of Chemical and Biological Engineering, Zhejiang University, Hangzhou 310058, China.*

^b *Institute of Zhejiang University-Quzhou, 99 Zheda Road, Quzhou 324000, China.*

*Corresponding Authors: yzhengl@zju.edu.cn; panpengju@zju.edu.cn

Measurements

Calculation of the Densities of Covalent and H-bonded Crosslinking Points.

According to the reaction stoichiometry and the crosslinked network structures, the densities of covalent (μ_c) and H-bond (μ_H) crosslinking points can be calculated from FTIR spectra results using the following equations:

$$\mu_c = \frac{\rho n_{\text{TREN}}}{n_{\text{TPAL}}M_{\text{TPAL}} + n_{\text{BAET}}M_{\text{BAET}} + n_{\text{TREN}}M_{\text{TREN}} - 2n_{\text{TPAL}}M_{\text{H}_2\text{O}}} \quad (\text{S1})$$

$$\mu_H = \frac{2f\rho n_{\text{BAET}}}{n_{\text{TPAL}}M_{\text{TPAL}} + n_{\text{BAET}}M_{\text{BAET}} + n_{\text{TREN}}M_{\text{TREN}} - 2n_{\text{TPAL}}M_{\text{H}_2\text{O}}} \quad (\text{S2})$$

where n_{TPAL} , n_{BAET} and n_{TREN} are the molar amounts of the TPAL, BAET and TREN monomers, respectively; M_{TPAL} , M_{BAET} , M_{TREN} and $M_{\text{H}_2\text{O}}$ are the molar masses of TPAL, BAET, TREN and H₂O, respectively; f is the fraction of the H-bond C=O groups in the PIMs (determined from FTIR spectra); and ρ is the density of the products (assumed to be 1.0 g/cm³).

Temperature-Dependent Fourier-Transform Infrared (FTIR) Spectroscopy.

Temperature-dependent FTIR spectra were performed on a Nicolet iS50 spectrometer (Thermo Fisher Scientific, USA) equipped with an MCT (HgCdTe) detector. The sample was prepared as a thin film on ZnSe slide and heated from 20 to 150 °C at a rate of 10 °C/min, during which the spectra was collected with a 10 °C interval. All spectra were collected with 32 scans in transmission mode at a resolution of 2 cm⁻¹.

Shape Memory Performance. Shape memory behavior was evaluated using a Q850 DMA (TA Instruments, USA). Rectangular specimens (15 mm in length, 5 mm in width, and ~0.15 mm in thickness) were cut from the PIM films. Each shape memory cycle was consisted of the following steps. 1) *Equilibration*: the sample was heated to 100 °C and held for 10 min under the zero-stress condition. 2) *Deformation and cooling*: A constant 10% strain (ϵ_{load}) was applied, and the sample was cooled to 25 °C while maintaining this strain. 3) *Stress removal and fixation*: At 25 °C, the stress was released, allowing the sample to relax to a temporary strain (ϵ). 4) *Recovery*: the sample was reheated to 100 °C under the zero-stress condition, recovering to a final strain (ϵ_{rec}). Both heating and cooling rates were 5 °C/min.

The shape fixity ratio (R_f) and shape recovery ratio (R_r) were calculated using the

following equations:

$$R_f = (\varepsilon / \varepsilon_{\text{load}}) \times 100\% \quad (\text{S3})$$

$$R_r = (1 - \varepsilon_{\text{rec}} / \varepsilon) \times 100\% \quad (\text{S4})$$

Supplementary Figures

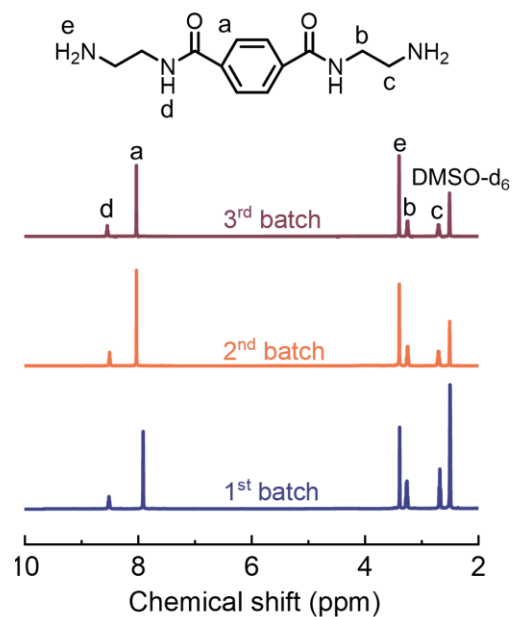


Figure S1. ^1H NMR spectrum of BAET obtained from three different batches of post-consumer PET bottles *via* aminolysis, using DMSO- d_6 as the solvent.

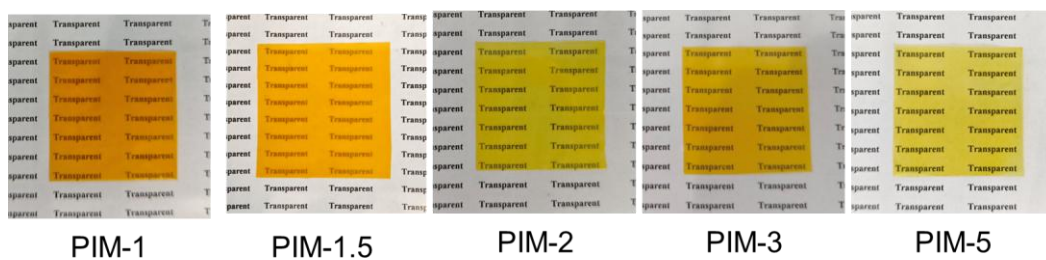


Figure S2. Photographs of PIM films with a thickness of ~ 0.15 mm.

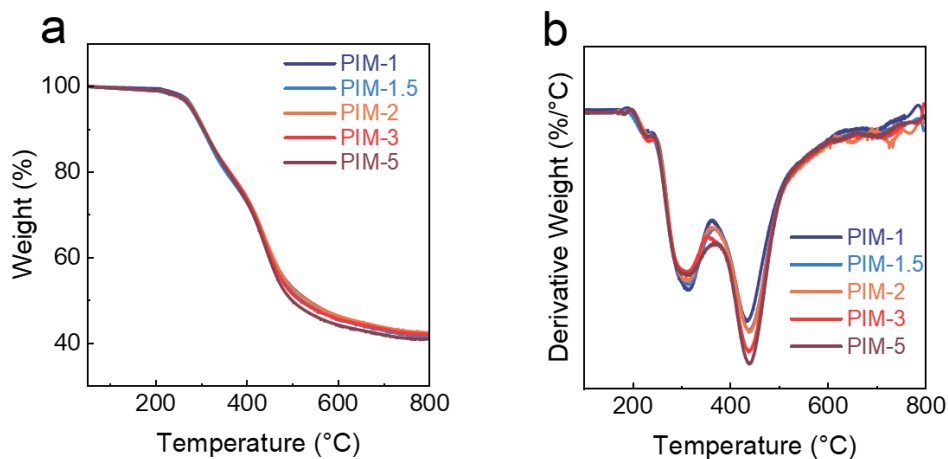


Figure S3. (a) TGA curves and (b) derivative weight curves of PIMs.

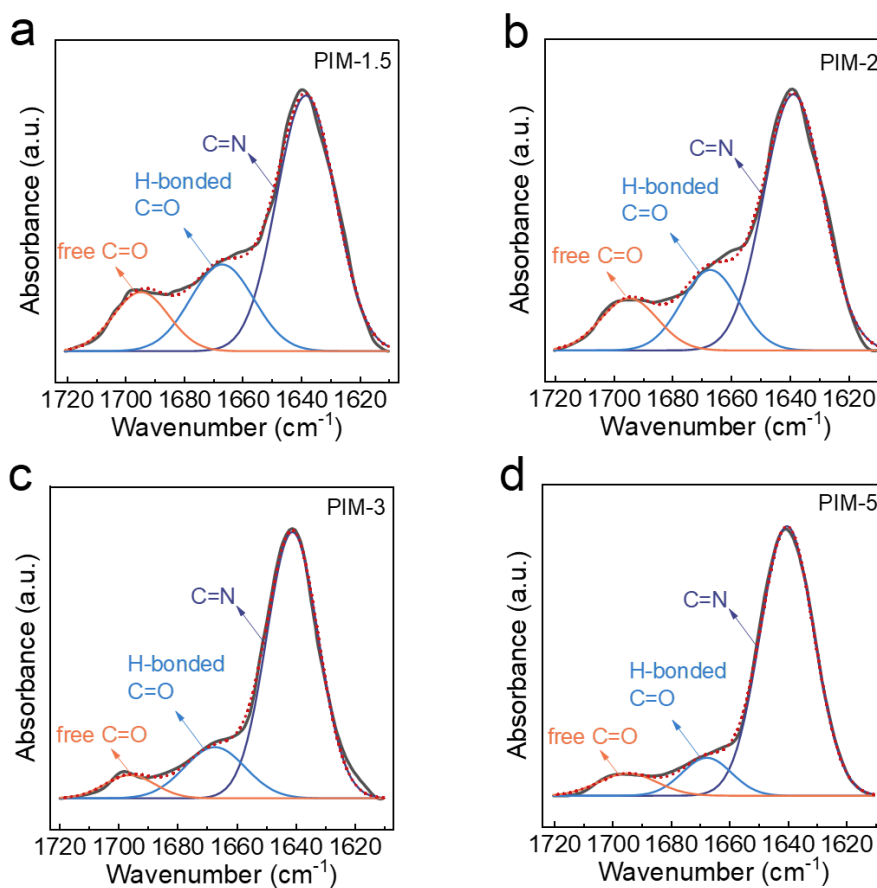


Figure S4. FTIR spectra of PIMs in the wavenumber range of 1720–1610 cm⁻¹ measured at 25 °C. (a) PIM-1.5; (b) PIM-2; (c) PIM-3; (d) PIM-5.

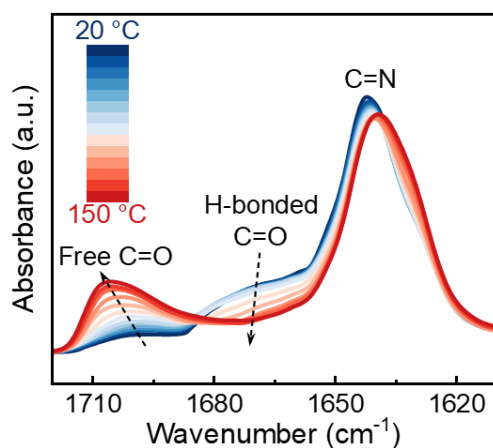


Figure S5. Temperature-dependent FTIR spectra of PIM-1.5 in the wavenumber range of 1720–1610 cm^{-1} collected upon heating from 20 to 150 $^{\circ}\text{C}$ at a rate of 10 $^{\circ}\text{C}/\text{min}$.

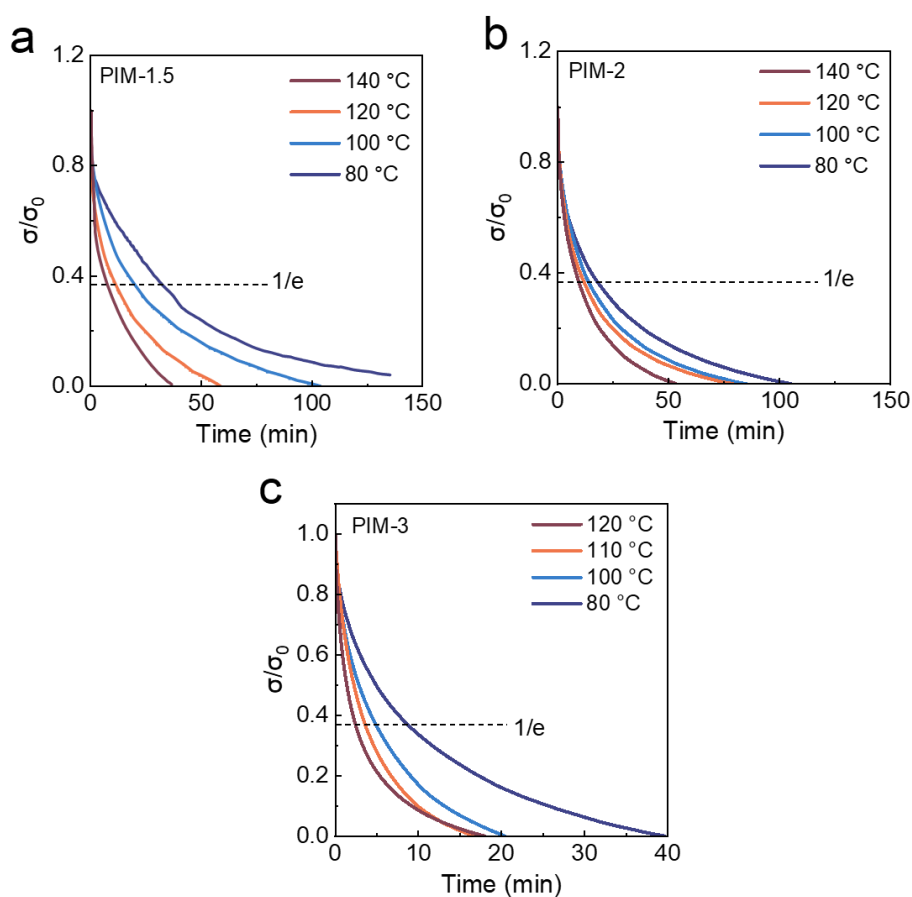


Figure S6. Normalized stress-relaxation curves of PIMs measured at different temperatures. (a) PIM-1.5; (b) PIM-2; (c) PIM-3.

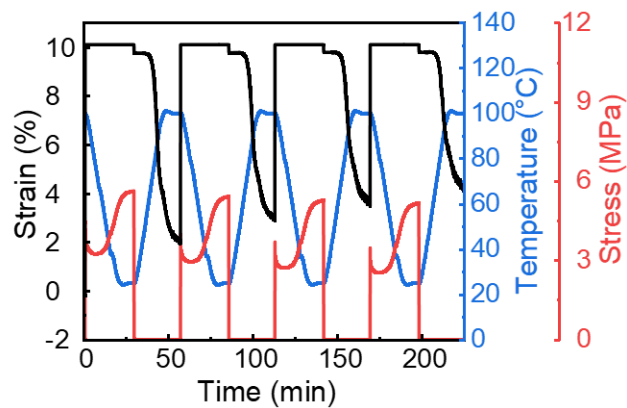


Figure S7. Shape memory performance of PIM-1.5 measured by DMA.

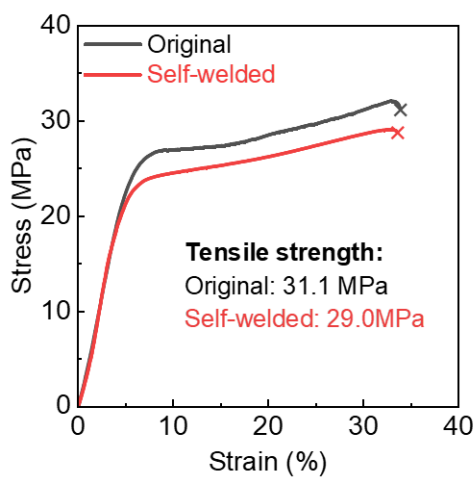


Figure S8. Engineering stress-strain curves of the original and self-welded PIM-1.5.

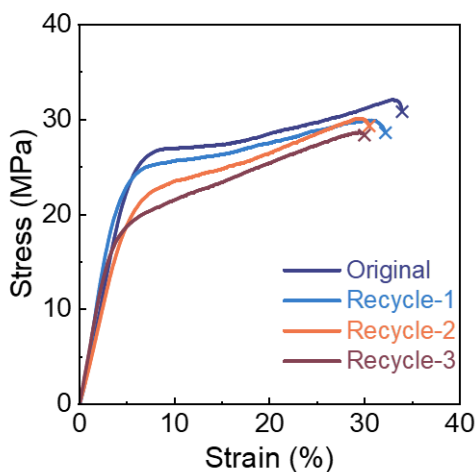


Figure S9. Engineering stress-strain curves of the original and chemically-recycled PIM-1.5 (in Figure 5c).

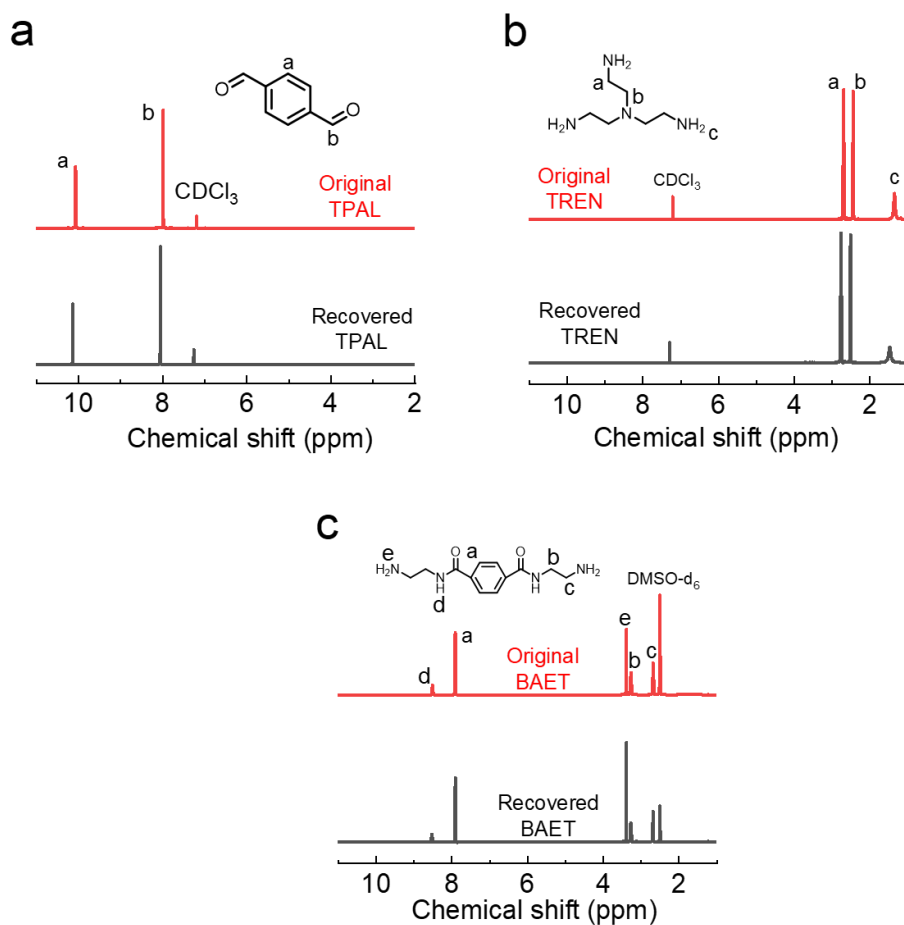


Figure S10. ^1H NMR spectra of original and recovered monomers. (a) Original and recovered TPAL; (b) original and recovered TREN; (c) original and recovered BAET.

Supplementary Tables

Table S1. Densities of covalent (μ_c) and H-bond (μ_H) crosslinking points calculated from FTIR spectra.

Sample	Covalent crosslinking points (μ_c , mmol/cm ³)	H-bond crosslinking points (μ_H , mmol/cm ³)
PIM-1	1.56	0.92
PIM-1.5	1.90	0.87
PIM-2	2.13	0.80
PIM-3	2.44	0.77
PIM-5	2.75	0.58

Table S2. Mechanical properties of PIMs calculated from engineering stress-strain curve in Figure 3a.

Sample	Young's modulus (MPa)	Tensile strength (MPa)	Elongation at break (%)
PIM-1	519.8 ± 22.2	36.6 ± 3.7	20.7 ± 1.7
PIM-1.5	490.3 ± 19.7	31.1 ± 2.4	33.9 ± 2.4
PIM-2	281.1 ± 18.1	21.3 ± 2.1	40.2 ± 2.7
PIM-3	151.6 ± 21.4	16.0 ± 2.0	43.9 ± 3.6
PIM-5	70.9 ± 5.6	8.7 ± 1.5	42.4 ± 2.9

Table S3. Mechanical properties of PIM-1.5 after multiple recycling cycles, as shown in Figure 5c.

Sample	Young's modulus (MPa)	Tensile strength (MPa)	Elongation at break (%)
Original	490.3 ± 19.7	31.1 ± 2.4	33.9 ± 2.4
Recycle-1	482.2 ± 18.6	29.3 ± 2.0	33.1 ± 1.9
Recycle-2	453.5 ± 18.9	28.6 ± 2.1	30.4 ± 2.6
Recycle-3	430.0 ± 15.1	30.1 ± 1.9	30.1 ± 2.7